Civil Engineering Research Magazine
CERM
ISSN 1110-0990
Vol., 46, 2025.

قياس الأعماق باستخدام تقنيات التعلم الآلي من صور القمر الصناعي سنتينل-2 لمنطقة جمشة على ساحل البحر الأحمر

Bathymetry Derived Using Machine Learning Techniques from Sentinel-2 Satellite Imagery of The Jemsha Region on The Red Sea Coast

Rania Hassan*[1], Ahmed Saber[2], Rasha Mohey El-Deen [2], Sameh ElKafrawy[3]and Mostafa Rabah[2]

1 Department of Civil Engineering, The Technological College in Quesna, Benha, Egypt.
2 Civil Engineering Department, Benha Faculty of Engineering, Benha University, Benha, Egypt.
3 Marine Sciences Department, National Authority for Remote Sensing, and Space Sciences (NARSS), Cairo, Egypt.
***Correspondence**: Rania.Moussa20@beng.bu.edu.eg

الملخص: قياس الأعماق مهم للعديد من الأنشطة مثل تطبيقات الهندسة الساحلية والمسوحات الهيدروغرافية. وقد وفرت صور الأقمار الصناعية تغطية واسعة النطاق وقياسات عمق منخفضة التكلفة وفعالة من حيث الوقت. في هذه الدراسة، تم استخدام بيانات الصور الفضائية سينتينال-2 لتقييم ثلاثة نماذج لحسابات العمق في منطقة جمشة بساحل البحر الأحمر علي ساحل خليج السويس. النماذج هي خوارزميات الشبكة العصبية الاصطناعية (ANN) ، وخوارزميات النموذج الإضافي المعمم (GAM) ، وخوارزميات تعزيز التدرج الأقصى (XGBOOST). النماذج المستخدمة للحصول على خرائط قياس الأعماق في المناطق الساحلية من صور الأقمار الصناعية سنتينال-2 استخدمت انعكاس النطاقات الحمراء والخضراء والزرقاء. نتج عن (ANN) قيمة RMSE تبلغ 1.054مترًا و R^2 تبلغ 0.948، ونتج عن (GAM) قيمة RMSE تبلغ 0.848 مترًا و R^2 تبلغ 0.966، ونتج عن (XGBOOST) قيمة RMSE تبلغ 0.942 مترًا و R^2 تبلغ 0.981على منطقة الدراسة. حقق نموذج المجموعة (EM) الذي يجمع بين GAM و XGBOOSTقيمةRMSE تبلغ 0.296 مترًا و R^2 تبلغ 0.966، مما يدل على الدقة المحسنة لتقنيات التعلم الآلي في رسم خرائط قياس الأعماق.

الكلمات المفتاحية: سينتينال-2؛ قياس الأعماق؛ التعلم الالي؛ نموذج المجموعة.

Abstract. Bathymetry is crucial for a variety of tasks, including hydrographic surveys and coastal engineering applications. The use of satellite images has made depth measurements quick, inexpensive, and widely available. Three models were evaluated in the current study for depth estimations in Jemsha, Red Sea Coast, the Gulf of Suez Coastline using Sentinel 2 satellite image data.. The models are Artificial Neural Network (ANN) algorithms, Generalized Additive Model (GAM) algorithms, and eXtreme Gradient BOOSTing (XGBOOST) algorithms. Models used to obtain bathymetry maps in coastal regions from sentinel-2 satellite images using red, green and blue bands reflectance. ANN resulted in RMSE 1.054 m and R^2 0.948, GAM produced RMSE 0.848 m and R^2 0.966, and XGBOOST produced RMSE. 0.942 m and R^2 0.981 over the study area. An Ensemble Model (EM) combining GAM and XGBOOST achieved an RMSE of 0.296 m and R^2 of 0.966, demonstrating the enhanced accuracy of ML techniques in bathymetric mapping.

Keywords: Sentinel-2, Bathymetry, Machine learning, Ensemble Model.

1. Introduction

For a variety of purposes, such as resource management and environmental monitoring, accurate bathymetric measurement is crucial in aquatic environments. Nonetheless, certain regions provide difficulties since they are hard to reach with conventional bathymetry techniques. The current research investigates the inference of bathymetry with Sentinel-2 satellite imagery and machine learning techniques. Since water makes up the majority of the Earth's surface, bathymetric mapping requires precise depth measurement. Although it requires a lot of time and money, classical hydrographic surveying with echo-sounders remains the most precise mapping technique for ocean floor and determining bathymetry [1]. Accurate seabed mapping is necessary for geoenvironmental studies, monitoring subsea power cables, and infrastructure development [2]. For safe maritime transit and navigation, especially in coastal and shallow water areas, up-to-date geospatial data is crucial. Accurate seabed knowledge is necessary for safe operations in ports, waterways, and jetties due to the dynamic nature of the seabed and potential threats from sedimentation. This highlights the importance of regular monitoring [1,3].

Conventional hydrography studies provide challenges, particularly in vast areas and coastal places where extensive and costly fieldwork is needed [2,3]. Coastal zones may have disruptions to continuous hydrography due to the seasonal monsoon system, making it challenging to maintain frequent surveys in certain areas. Complexity and potential risk are increased when shorelines, ecosystems, and environs are explored in rocky-cliff zones utilising sounding boats. However, remote multispectral sensors aboard satellites offer a cost-effective solution for continuous earth observation and shallow water bathymetry, with revisit intervals of a few days or weeks [4, 5], [6]. Since going into operation in 2014, Sentinel-2 has been taking pictures in 13 different electromagnetic spectrums and releasing the images publicly with a 10-day revisit interval and a 10-to 60-meter spatial resolution. Similarly, a nine-band dataset having a 16-day temporal resolution and a saptial resolution of 15–30 meters is offered by Landsat-8 OLI, which has been in operation since 2013. The relationship between electromagnetic properties and light penetration allows bathymetry to be estimated from satellite data, especially Sentinel-2 and Landsat-8 [6, 7].

Among the satellite sensors whose bathymetry estimation has been assessed are SPOT6, Sentinel-2, Landsat-8, and IKONOS. The parameters that impact the accuracy of remote sensing data include the reflection of water surface, atmospheric impacts, the reflection of sun, depth range, water quality, image pixel size, seabed characteristics, and sample placements [2, 3, 8]. By using complex algorithms, water reflectance ratio models, and radiometric correction methods to overcome issues with satellite-derived bathymetry, researchers have drawn attention from the scientific community [9].

Artificial Neural Networks (ANN), Random Forests (RF), and Support Vector Machines (SVM) are examples of machine learning (ML) and statistical techniques that have shown efficacy in the efficient analysis of multi-dimensional satellite datasets for tasks like image classification and bathymetry obtained from satellites. [2, 5, 8]. While a number of machine learning techniques have demonstrated potential for obtaining depth data in transparent and shallow waters, further investigation is required to improve the precision and stability of the depth of water retrieval when utilizing complex algorithms such as the GBM, Catboost, and XGboost models. Machine learning algorithms' inherent "black box" nature has made interpretability and explainability necessary, necessitating the development of eXplainable artificial intelligence (XAI) [4,8,10].

In the current study, high-resolution satellite data from Sentinel-2 is used to evaluate bathymetry using potent machine learning approaches (ANN, GAM, and XGBOOST). To verify accuracy, these approaches' performance is contrasted with field bathymetric data.

2. Study Area and Data Sources

2.1. Area of Study

Located in the Gulf of Suez and along the Red Sea coast, the study site is about 60 kilometres from Hurghada and near to Jemsha, Egypt. It's a tourist location and a tiny bay. There is an oil refinery and oil field nearby, which occasionally results in oil leaks. The location is depicted in **fig.1**. The coordinates are as follows: Latitude: 27°38'N to 27°39'N; longitude: 33°33'E to 33°35'E.

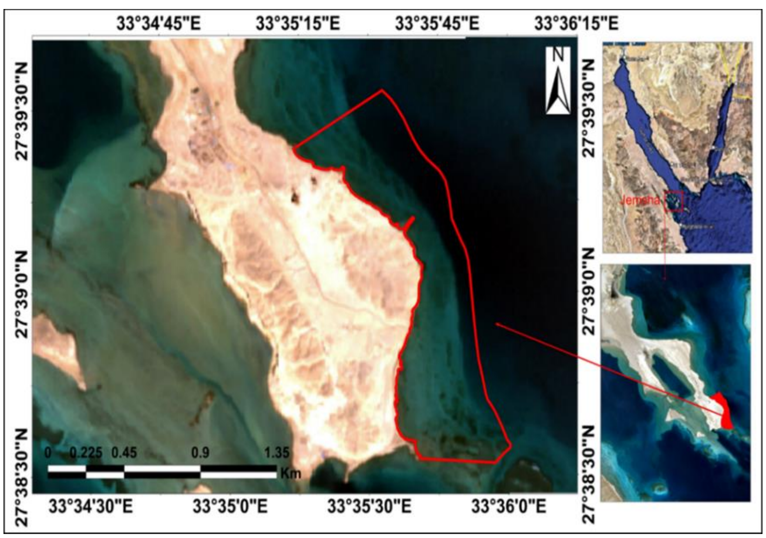

Fig.1: The Study Area Location: Jemsha, Gulf of Suez Coastline, Red Sea Coastline.

2.2. Satellite Data

The bathymetry data needed for the current study was obtained using an image from the Sentinel-2 satellite. August 2022 time scenes that were nearest to each other were chosen.

2.2.1 Sentinel-2 Image

Sentinel-2 Level 2A spacecraft processes images to give surface reflectance data and correct for air factors. They can be useful for mapping land cover, monitoring vegetation, assessing water quality, and disaster management, among other applications.
The data used in this investigation came from [11].

2.3. Field Data (Echo Sounder)

As part of a field campaign to map the coastal and marine areas, which extend up to 200 meters from the shoreline, modern bathymetry and sonar equipment has been deployed in the Jemsha region to ascertain the topography and depth of the sea floor for the study area. This map is shown in **fig 2.**
A depth gradient is depicted on the bathymetric map, with a maximum depth of eighteen meters. The tongue region is particularly shallow, with depths between one and two meters. This region's sea floor is level and devoid of notable topographical features. Additional examination indicates that the topography is unclear, and that the bottom edge grows noticeably steeper beyond 7 meters, creating a deep area that runs parallel to the shoreline.

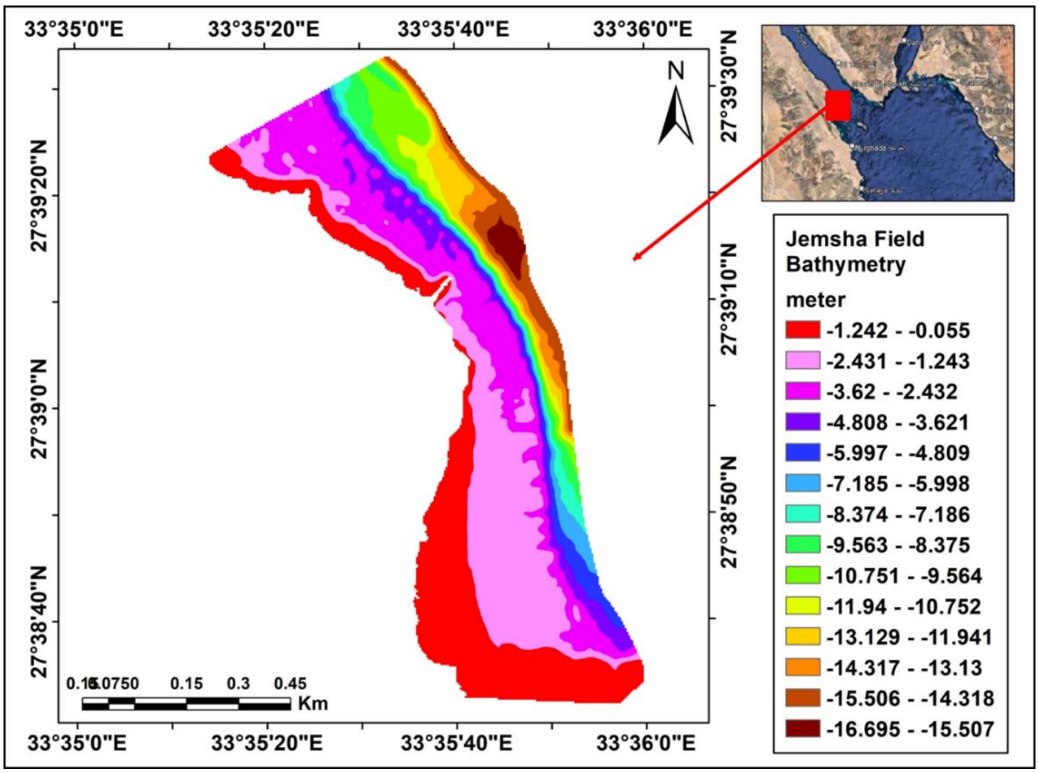

Fig. 2: Jemsha Field Bathymetric Map.

3. Methodology

3.1. Bathymetric Extraction Workflow Steps

The steps below were used to get bathymetry using machine learning approaches:
1 - Sentinel-2 Level 2A corrected reflectance images provided three inputs, which were used to train all approaches at the same field measurement point position. The logarithms of the red, green, and blue bands which represented the detected water depths were the outputs.
2 - These values were randomly split into independent 80% training and 20% testing points for the study area.
3 - In the end, the same independent testing points based on RMSE and R^2 values were used to evaluate all results from different methodologies.
The workflow for the bathymetry detection steps is shown in **fig. 3.**

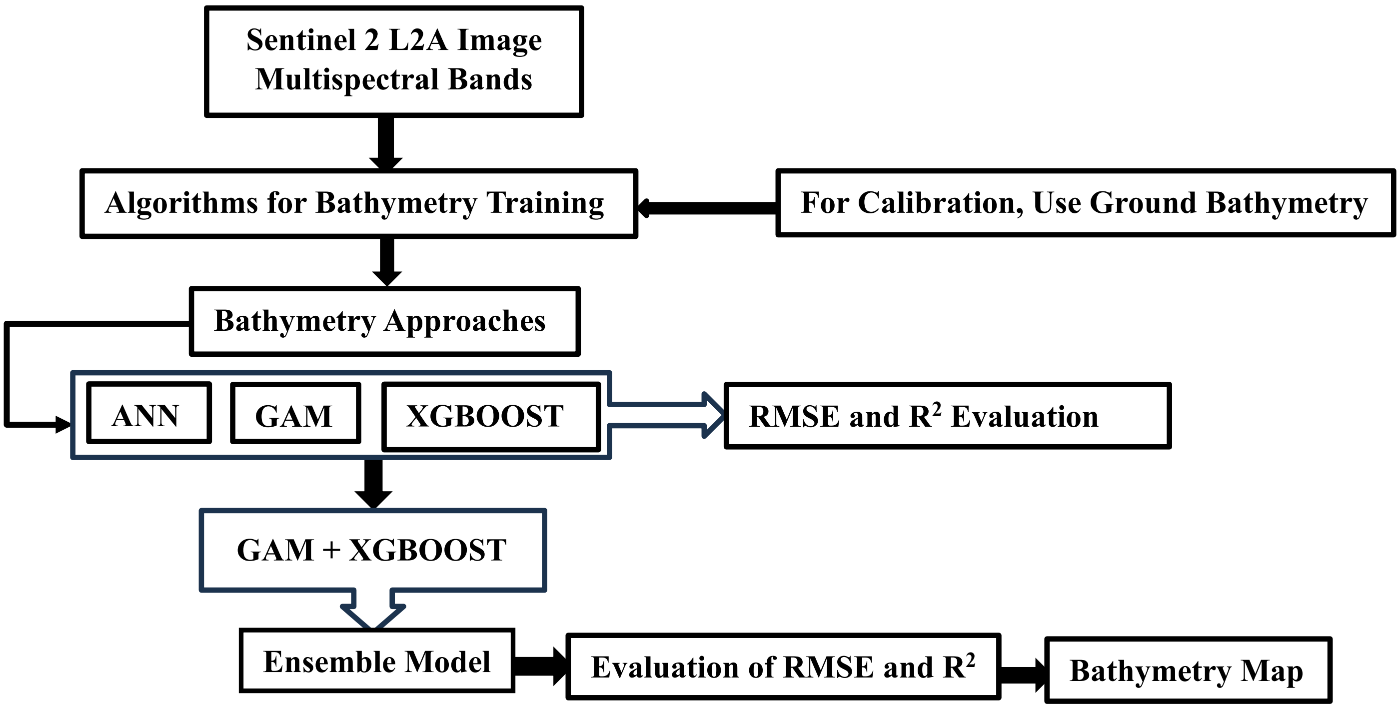

Fig. 3: Workflow of Study Area Bathymetry Detection Steps.

3.2. Machine Learning Models for Extracting Bathymetry

The current work used three supervised learning techniques to map bathymetry. These advanced Machine Learning (ML) techniques, include ANN, GAM, and XGBOOST for satellite-derived bathymetry, are briefly described after.

3.2.1 Artificial Neural Network (ANN)

Layers of artificial neurones, known as units, contribute to artificial neural networks (ANNs). Depending on the complexity needed to uncover hidden patterns in the dataset, these layers can have a number ranging from few units to millions. An ANN normally consists of an output layer, hidden layers, and an input layer. The output layer gives the network's answer after the input layer receives data that has been altered by the hidden layers [12].
Units in neural networks are interconnected, with each connection having weights that influence the units. As data transfers between units, the network learns and produces an output [13].
This research uses the Multilayer Feed-Forward (Multilayer Perceptron, MLP) Neural Network Algorithm, a supervised approach for mapping input to output data [14]. MLP has three parts: input layers (multispectral image band values), hidden layers (training process), and output layers (bathymetric information). A hypothetical example of an MLP with 4 input layers, 5 hidden layers, and 1 output layer (4-5-1) is shown in **fig. 4.**

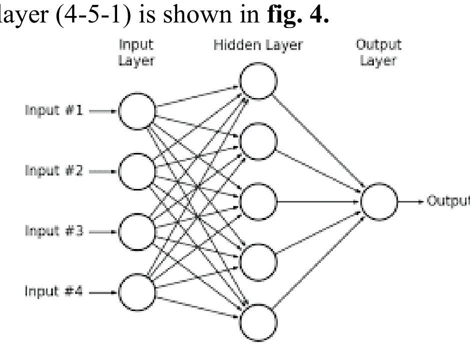

Fig.4 Hypothetical example of a Multilayer Perceptron Network.

Rectified Linear Unit (ReLU) activation functions are used for hidden layers, and a linear activation function is used for the output layer. ReLU, defined as $f(x) = max\ (0, x)$, is effective in preventing the vanishing gradient problem [15]. The linear activation function for the output layer is $f(x) = x$ [16].

The Adam optimizer was used for updating weight and bias values, combining RMSprop and momentum methods. It maintains two moving averages: the first moment (mean) and the second moment (uncentered variance) of the gradients. The equations for Adam are listed (from (1) to (5)):

- Compute gradients of the loss function.
- Update biased first moment estimate in Equation 1

$$m_t = \beta_1 \cdot m_{t-1} + (1-\beta_1) \cdot gt \qquad (1)$$

- Update biased second raw moment estimate in Equation 2

$$v_t = \beta_2 \cdot v_t - 1 + (1-\beta_2) \cdot g_t^2 \qquad (2)$$

- Bias-corrected first moment estimate in Equation 3

$$\acute{m}t = \frac{m_t}{1-\beta_1^t} \qquad (3)$$

- Bias-corrected second raw moment estimate in Equation 4

$$\grave{v}t = \frac{v_t}{1-\beta_2^t} \qquad (4)$$

- Update parameters in Equation 5

$$\varpi_{t+1} = \varpi_t - \frac{\eta}{\sqrt{\grave{v}_t + \epsilon}} \cdot m_t \qquad (5)$$

These equations update the network's weights and biases using the Adam optimization algorithm. All algorithms and statistical analyses were implemented in Python.

3.2.2. Generalized Additive Model (GAM)

By permitting nonlinear interactions between the dependent and independent variables, a Generalised Additive Model (GAM) expands on linear regression. Unlike linear regression, which assumes a linear relationship, GAMs use smooth functions to capture complex relationships [17].

The general form of a GAM is as shown in Equation 6:

$$Y = \beta_0 + f_1(X_1) + f_2(X_2) + \ldots + f_p\ (X_p) + \epsilon \qquad (6)$$

where: The dependent variable, or response, is $Y, X_1, X_2 \ldots, X_p$ are the independent variables (predictors), The term that intercepts is β0, f1, f2…, fp are smooth functions of the predictors and ϵ represents the error term [18].

In a GAM, each predictor Xi is associated with a smooth function fi (Xi), modelled using techniques like splines, local regression, or kernel smoothing. These smooth functions capture nonlinear relationships, making GAMs highly flexible.

The smooth functions fi (Xi) are often estimated using penalized regression techniques, such as penalized splines or generalized cross-validation, to prevent overfitting and ensure interpretability [19]. The degree of smoothness is controlled by tuning parameters or penalties, selected using techniques like cross-validation.

GAMs are widely used in fields like epidemiology, environmental science, and econometrics, where relationships between variables may be nonlinear or non-monotonic [18].

They provide a powerful framework for modelling complex data relationships while maintaining interpretability and ease of use.These algorithms and statistical analyses were implemented in Python.

3.2.3. Extreme Gradient Boosting (XGBOOST)

EXtreme Gradient BOOSTing (XGBOOST), is understood through its mathematical formulation, particularly its optimization objective and update algorithm.**Objective Function** [20]: XGBoost minimizes a regularized objective function combining a loss function with regularization terms, as shown in Equation 7:

$$Obj(\theta) = \sum_{i=1}^{n} loss(y_i\ , \bar{y}_i) \quad + \sum_{k=1}^{K} \Omega(f_k) \qquad (7)$$

where: Obj(θ) is the overall objective function, θ represents model parameters, n denote to the number of training instances, yi is the true label, ȳi is the predicted label, loss , $loss(y_i\ , \bar{y}_i)$ measures the difference between true and predicted labels, K is the number of trees and Ω (fk) is the regularization term.

Loss Function [21]: The loss function depends on the problem type (e.g., regression), commonly using Squared Loss (MSE) for regression: loss $loss(y_i\ , \bar{y}_i) = (y_i - \bar{y}_i)^2$.

Regularization Terms: To manage model complexity, XGBOOST uses L1 (Lasso) and L2 (Ridge) regularisation:

- L1 Regularization (Lasso): $\Omega(fk) = \lambda 1 \sum_{j=1}^{T} \mid w_j \mid$.
- L2 Regularization (Ridge): $\Omega(fk)=\lambda 2 \sum_{j=1}^{T} w_j^2$.

where: λ1 and λ2 are the regularization parameters, T is the number of leaves in the tree, wj are the weights associated with each leaf.
Tree Update: In each iteration, a new tree is added, and leaf weights are updated to minimize the objective function. Optimal leaf scores are calculated as in Equation 8:

$$\gamma_j^* = -\frac{G_j}{H_{j+\lambda_2}} \tag{8}$$

Where: γ_j^* is the optimal weight for the j-th leaf, Gj and Hj are the loss function's first and second-order gradients in relation to the forecasts at the j-th leaf, respectively.
These equations illustrate XGBOOST's combination of gradient boosting and regularization to build robust predictive models. XGBOOST is a powerful tool for accurate predictive modelling, implemented in Python for statistical analysis.

3.2.4. Ensemble Model (EM)

EXtreme Gradient BOOSTing (XGBOOST) and the Generalized Additive Model (GAM) were combined to improve accuracy because these two models produced the best results when bathymetry was estimated from multispectral satellite pictures.

4. Results

In the current study, bathymetry was estimated using three machine learning techniques and an ensemble model approach using high-resolution data from Sentinel-2 satellites. Below are the outcomes of several machine learning approaches, including ANN, GAM, XGBOOST, and EM.
The precision of the employed methods can be summed up as follows:
ANN, GAM and XGBOOST give RMSE values of 1.054 m, 0.848 m, and 0.942 m, and R2 of 0.948, 0.966 and 0.981, respectively.
To further optimize accuracy, the advantages of the GAM and XGBOOST were combined to produce an Ensemble Model (EM). The findings of this ensemble model indicated improved accuracy, a reduced RMSE of 0.296 m, and an R2 of 0.966, proving the value of combining models for depth inference while taking measurements of depth in coastal areas.

4.1. Depth Estimation

The ANN uses ReLU activation to avoid vanishing gradients and a linear function in the output layer after being trained with the Levenberg-Marquardt back-propagation function with ten hidden layers. The Adam optimizer, combining RMSprop and momentum methods, updates network parameters iteratively, enhancing training convergence. The GAM forecasts depths from satellite data using smooth functions of predictors and an error term, with smoothing controlled by the lambda parameter. A lambda of 0.1 to 1.0 and 20 splines per feature balance complexity and overfitting, with values between 10 to 50 being reasonable depending on data complexity. The XGBOOST algorithm limits the number of boosting rounds to 100 and uses step size shrinkage to prevent overfitting. At a lower number, the model is more resilient, but additional boosting cycles are required. The value of it is 0.1.
However, the lowest Root Mean Square Error (RMSE) and the highest correlation coefficient-squared (R2) values were taken into consideration when choosing the parameters of each algorithm. Higher R2 and lower RMSE indicate a better fit between the model and the data. Python was the programming language used for all statistical analysis and procedures. While the estimation and bathymetric maps for each model are shown in Figs. 5 and 6, respectively, Table 1 briefly presents the associated values of RMSE and R^2.

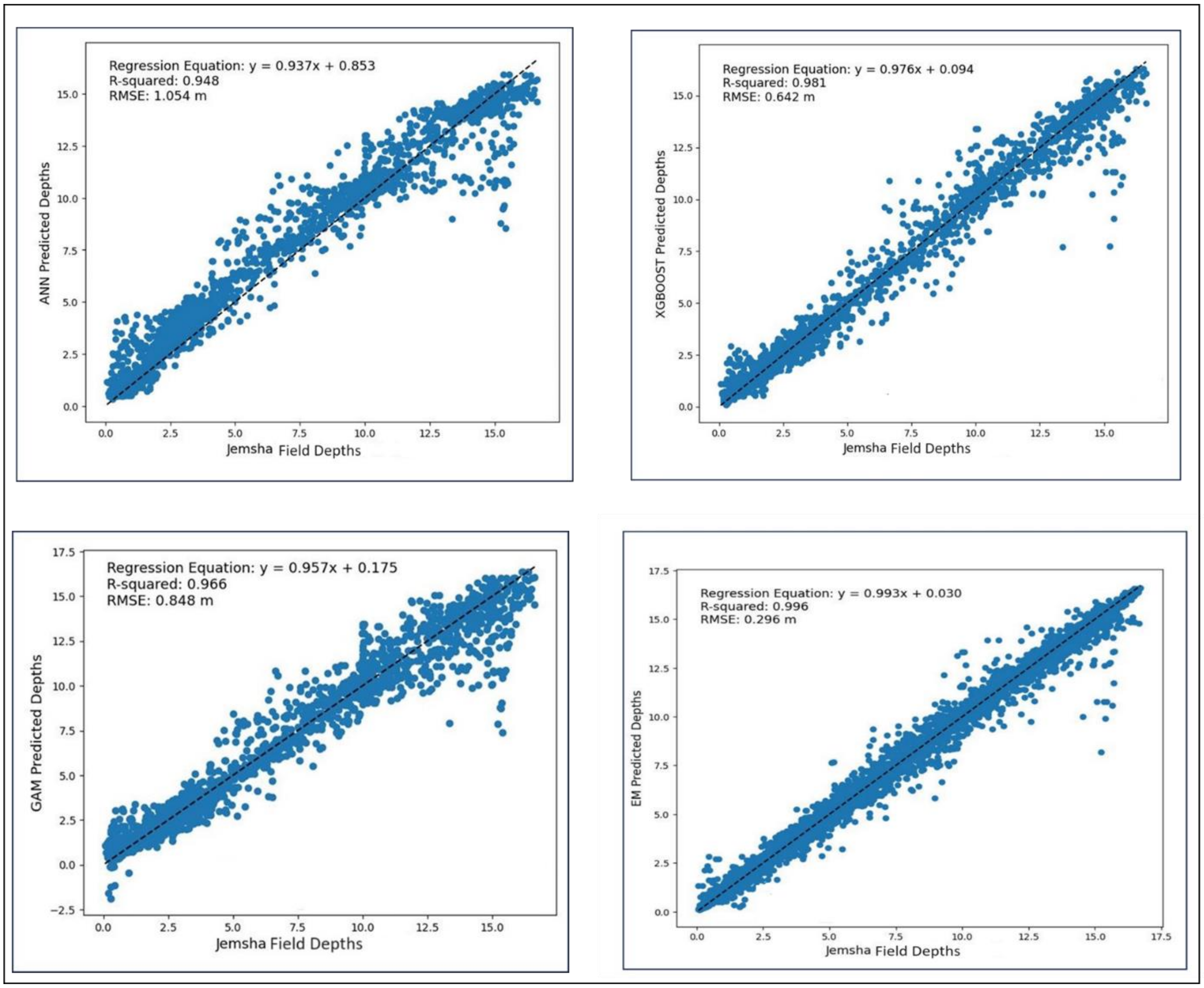

Fig. 5 Constantly Fitted Models for Machine Learning Model Techniques.

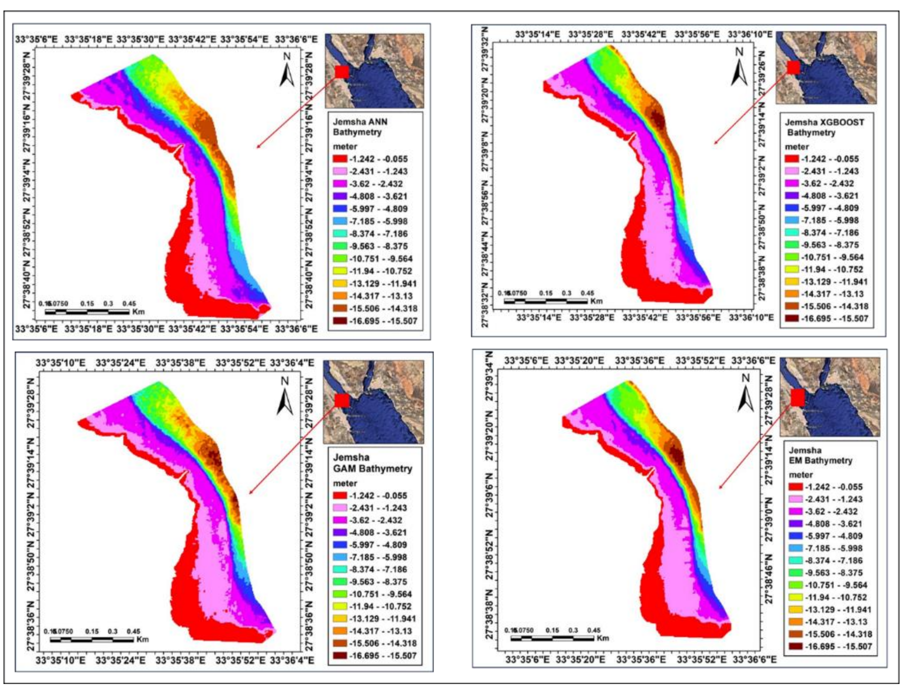

Fig.6 Bathymetric Map Utilizing Machine Learning Modeling Techniques.

Table 1: RMSE and R^2 for the Study Area's Bathymetric Value Checking Parameters

Methodology	ANN	GAM	XGBOOST	EM
RMSE (m)	1.054	0.848	0.942	0.296
R^2	0.948	0.966	0.981	0.966

5. Discussion

The comparison between the algorithms of the red, green, and blue bands was the most insightful addition to the present study. The final results are summarized as follows:
In ANN, trained with the Levenberg-Marquardt back-propagation function and featuring ten hidden layers, uses ReLU activation to avoid vanishing gradients and a linear function in the output layer. The Adam optimizer, which merges RMSprop and momentum methods, updates network parameters iteratively to improve training convergence.
In GAM predicts depths from satellite data by using smooth functions of predictors and an error term, with smoothing adjusted by the lambda parameter. A lambda range of 0.1 to 1.0 and 20 splines per feature balance complexity and overfitting, with 10 to 50 splines being reasonable based on data complexity.
The XGBOOST algorithm limits the number of boosting rounds to 100 and use step size shrinkage to prevent overfitting. A typical value of 0.1 indicates that the model is more robust at lower values, but more boosting rounds are required.
Finally, to improve overall predictive performance, the EM approach demonstrates how to build an ensemble by combining predictions from XGBOOST and GAM. According to the findings, XGBOOST and GAM outperform ANN in the researched field in terms of accuracy.

6. Conclusions And Recommendations

Current research demonstrates the potential of using Sentinel-2 satellite imagery and machine learning algorithms to infer water depths in coastal areas.
The results of the Ensemble Model (EM) used in the study indicated improved accuracy, demonstrating the importance of integrating machine learning models with superior results for inferring depth when be measured in coastal areas.
Further research and validation in other aquatic environments are recommended to improve the flexibility and applicability of the proposed approach.

Acknowledgments. The authors wish to acknowledge the support of civil engineering department, Benha Faculty of Engineering, Benha University, Benha, Egypt.

Conflict of Interest. Regarding the content of this essay, the authors have no financial interests to disclose.

References

[1] Sam-Khaniani A., Viccione G., Qorbani Fouladi M., and Hesabi-Fard R., “Analysis of Dynamic Changes in Sedimentation in the Coastal Area of Amir-Abad Port Using High-Resolution Satellite Images,” *J Imaging*, vol. 11, no. 3, p. 86, Mar. 2025, doi: 10.3390/jimaging11030086.

[2] Evagorou E., Argyriou A., Papadopoulos N., Mettas C., Alexandrakis G., and Hadjimitsis D., “Evaluation of Satellite-Derived Bathymetry from High and Medium-Resolution Sensors Using Empirical Methods,” *Remote Sens (Basel)*, vol. 14, no. 3, p. 772, Feb. 2022, doi: 10.3390/rs14030772.

[3] Jagalingam P., Akshaya B. J., and Hegde A. V., “Bathymetry Mapping Using Landsat 8 Satellite Imagery,” *Procedia Eng*, vol. 116, pp. 560–566, 2015, doi: 10.1016/j.proeng.2015.08.326.

[4] Philpot W. D., “Bathymetric mapping with passive multispectral imagery,” *Appl Opt*, vol. 28, no. 8, p. 1569, Apr. 1989, doi: 10.1364/AO.28.001569.

[5] Stumpf R. P., Holderied K., and Sinclair M., “Determination of water depth with high-resolution satellite imagery over variable bottom types,” *Limnol Oceanogr*, vol. 48, no. 1part2, pp. 547–556, Jan. 2003, doi: 10.4319/lo.2003.48.1_part_2.0547.

[6] Muhammad F., Tsimpouxis I., and Sternberg H., “Investigating the Impact of Spatiotemporal Variations in Water Surface Optical Properties on Satellite-Derived Bathymetry Estimates in the Eastern Mediterranean,” *Remote Sens (Basel)*, vol. 17, no. 3, p. 444, Jan. 2025, doi: 10.3390/rs17030444.

[7] Mavraeidopoulos A. K., Oikonomou E.,. Palikaris A, and Poulos S., “A Hybrid Bio-Optical Transformation for Satellite Bathymetry Modeling Using Sentinel-2 Imagery,” *Remote Sens (Basel)*, vol. 11, no. 23, p. 2746, Nov. 2019, doi: 10.3390/rs11232746.

[8] Kamal N. and El-Ashmawy N., “Potential of Using Machine Learning Regression Techniques to Utilize Sentinel Images for Bathymetry Mapping of Nile River,” *The Egyptian Journal of Remote Sensing and Space Sciences*, vol. 26, no. 3, pp. 545–555, Dec. 2023, doi: 10.1016/j.ejrs.2023.06.004.

[9] Lyzenga D. R., “Passive remote sensing techniques for mapping water depth and bottom features,” *Appl Opt*, vol. 17, no. 3, pp. 379–383, 1978.

[10] Dey M., Som K. S., Nandy S., and Chavan S. B., “Generation of site-specific nearshore bathymetry algorithms using remote sensing and GIS: a case study of Southern coastal regions of India,” *Discover Oceans*, vol. 2, no. 1, p. 6, Feb. 2025, doi: 10.1007/s44289-025-00047-8.

[11] “https://dataspace.copernicus.eu.”

[12] Hopfield J. J., “Neural networks and physical systems with emergent collective computational abilities.,” *Proceedings of the National Academy of Sciences*, vol. 79, no. 8, pp. 2554–2558, Apr. 1982, doi: 10.1073/pnas.79.8.2554.

[13] Macukow B., “Neural Networks – State of Art, Brief History, Basic Models and Architecture,” 2016, pp. 3–14. doi: 10.1007/978-3-319-45378-1_1.

[14] Smolensky P., *Mathematical Perspectives on Neural Networks*. Psychology Press, 2013. doi: 10.4324/9780203772966.

[15] Nair G. H. V, “Rectified Linear Units Improve Restricted Boltzmann Machines,” in *the 27th international conference on machine learning*, Canada, 2010.

[16] Xavier Glorot Y. B., “Understanding the difficulty of training deep feedforward neural networks,” in *the 13th International Conference on Artificial Intelligence and Statistics (AISTATS)*, Sardinia, Italy, 2010, pp. 249–256.

[17] Wölfl A.-C. *et al.*, “Seafloor Mapping – The Challenge of a Truly Global Ocean Bathymetry,” *Front Mar Sci*, vol. 6, Jun. 2019, doi: 10.3389/fmars.2019.00283.

[18] Wood S. N., *Generalized Additive Models*. Chapman and Hall/CRC, 2017. doi: 10.1201/9781315370279.

[19] Trevor J. Hastie, *Statistical Models in S*, 1st ed. 19992.

[20] Chen T. and Guestrin C., “XGBoost,” in *Proceedings of the 22nd ACM SIGKDD International Conference on Knowledge Discovery and Data Mining*, New York, NY, USA: ACM, Aug. 2016, pp. 785–794. doi: 10.1145/2939672.2939785.

[21] Friedman J. H., “Greedy function approximation: A gradient boosting machine.,” *The Annals of Statistics*, vol. 29, no. 5, Oct. 2001, doi: 10.1214/aos/1013203451.